PREPRINT 450

APRIL 2016

L^2-Error Analysis of an Isoparametric Unfitted Finite Element Method for Elliptic Interface Problems

Christoph Lehrenfeld* and Arnold Reusken†

Institut für Geometrie und Praktische Mathematik
Templergraben 55, 52062 Aachen, Germany

* Institut für Numerische und Angewandte Mathematik, WWU Münster, D-48149 Münster, Germany; email: lehrenfeld@uni-muenster.de
† Institut für Geometrie und Praktische Mathematik, RWTH Aachen University, D-52056 Aachen, Germany; email: reusken@igpm.rwth-aachen.de

L^2-ERROR ANALYSIS OF AN ISOPARAMETRIC UNFITTED FINITE ELEMENT METHOD FOR ELLIPTIC INTERFACE PROBLEMS

CHRISTOPH LEHRENFELD* AND ARNOLD REUSKEN†

Abstract. In the context of unfitted finite element discretizations the realization of high order methods is challenging due to the fact that the geometry approximation has to be sufficiently accurate. Recently a new unfitted finite element method was introduced which achieves a high order approximation of the geometry for domains which are implicitly described by smooth level set functions. This method is based on a parametric mapping which transforms a piecewise planar interface (or surface) reconstruction to a high order approximation. In the paper [C. Lehrenfeld, A. Reusken, *Analysis of a High Order Finite Element Method for Elliptic Interface Problems*, arXiv 1602.02970, Accepted for publication in IMA J. Numer. Anal.] an a priori error analysis of the method applied to an interface problem is presented. The analysis reveals optimal order discretization error bounds in the H^1-norm. In this paper we extend this analysis and derive optimal L^2-error bounds.

Key words. unfitted finite element method, isoparametric finite element method, high order methods, geometry errors, interface problems, Nitsche's method

AMS subject classifications. 65M06, 65D05

1. Introduction. In recent years there has been a strong increase in the research on development and analysis of *unfitted finite element methods*, cf. for example [1, 5, 8, 15, 16, 17, 19, 27]. The design, realization and analysis of unfitted finite elements methods which are *higher order* accurate is a challenging task. Especially in a setting where geometries are only implicitly described, e.g. by a zero level of a level set function, accurate numerical integration is difficult. Different techniques have been developed to overcome this difficulty [29, 26, 32, 30, 6, 9, 12, 3, 5, 14]. For a further discussion of the relevant literature we refer to [24, Section 1.2].

Recently, in [22], we introduced a new high order unfitted finite element method for scalar interface problems based on isoparametric mappings which is suitable for level set descriptions and higher order unfitted finite elements. The method is geometry based and is applicable to a wide range of problems, e.g. Stokes interface problems [21], fictitious domain problems [23] or surface PDEs [13].

A detailed a-priori error analysis of the method applied to a scalar elliptic interface model problem is given in [24]. Optimal H^1-norm discretization error bounds are derived for the case of a polygonal domain. In this paper we consider the same elliptic interface problem as in [24] and extend the existing analysis in two directions. First, we allow for a *piecewise smooth*, not necessarily polygonal, *domain*, which is approximated with a higher order isoparametric boundary approximation. Secondly, we complement the existing analysis with *optimal L^2-estimates*.

The paper is organized as follows. In Section 2 we introduce the model interface problem. We assume a level set description of the interface and discuss a standard piecewise planar interface approximation in Section 3. A key ingredient in the higher order unfitted finite element method is the isoparametric mapping used to obtain higher order geometry approximations. In Section 4 we present the construction of this mapping and the isoparametric unfitted finite element method for the elliptic

*Institut für Numerische und Angewandte Mathematik, University of Göttingen, D-37083 Göttingen, Germany; email: lehrenfeld@math.uni-goettingen.de

†Institut für Geometrie und Praktische Mathematik, RWTH Aachen University, D-52056 Aachen, Germany; email: reusken@igpm.rwth-aachen.de

interface problem. In particular it is explained how the same extension technique, which is a standard component in isoparametric finite element methods for high order approximation of smooth boundaries, is applied both for the boundary and interface mesh transformation. A main contribution of this paper is the error analysis of the method, i.e. the derivation of optimal H^1- and L^2-error bounds. The H^1-error results obtained in [24] (for a polygonal domain) form the basis for this analysis. In Section 5 we recall the most important results from [24] and adapt these to the case of a higher order isoparametric boundary approximation. The L^2 error analysis is presented in Section 6. Finally, in Section 7 we give results of a numerical experiment.

We are aware of the fact that parts of the paper contain results that are essentially the same as in [24]. In particular the material given in the sections 3, 4.1, 4.2 and 4.4 can also be found in [24]. We decided to include this material to make this paper more self-contained and thus improve its readability.

2. Model interface problem. We consider the model problem

$$-\mathrm{div}(\alpha_i \nabla u) = f_i \quad \text{in} \;\; \Omega_i, \; i = 1,2, \tag{2.1a}$$

$$[\![\alpha \nabla u]\!]_\Gamma \cdot n_\Gamma = 0, \quad [\![u]\!]_\Gamma = 0 \quad \text{on} \;\; \Gamma, \tag{2.1b}$$

$$u = 0 \quad \text{on } \partial\Omega. \tag{2.1c}$$

Here, $\Omega_1 \cup \Omega_2 = \Omega \subset \mathbb{R}^d$, $d = 2,3$, is a nonoverlapping partitioning of the domain, $\Gamma = \overline{\Omega}_1 \cap \overline{\Omega}_2$ is the interface and $[\![\cdot]\!]_\Gamma$ denotes the usual jump operator across Γ. The source terms f_i are given on each subdomain Ω_i, $i = 1,2$. In the remainder we also use the source term f on Ω which we define as $f|_{\Omega_i} = f_i$, $i = 1,2$. We assume Γ to be characterized as the zero level of a level set function (not necessarily a distance function). The diffusion coefficient α is assumed to be piecewise constant, i.e. it has a constant value $\alpha_i > 0$ on each sub-domain Ω_i. The weak formulation of this problem is as follows: determine $u \in H_0^1(\Omega)$ such that

$$\int_\Omega \alpha \nabla u \cdot \nabla v \, dx = \int_\Omega f v \, dx \quad \text{for all} \;\; v \in H_0^1(\Omega).$$

In the error analysis we assume that $\overline{\Omega}_1$ is strictly contained in Ω, i.e., $\Gamma = \partial\Omega_1$ and $\mathrm{dist}(\Gamma, \partial\Omega) > 0$. Furthermore, we assume Γ to be (globally) smooth and $\partial\Omega$ to be piecewise smooth.

3. Boundary parametrization and level set representation of the interface. The domain Ω, which has a (piecewise) smooth boundary is approximated with a family of *polygonal* approximations $\{\Omega_h^{\mathrm{lin}}\}_{h>0}$ corresponding to a family $\{\mathcal{T}_h\}_{h>0}$ of simplicial shape regular triangulations of $\{\Omega_h^{\mathrm{lin}}\}_{h>0}$ which are not fitted to Γ, cf. Fig. 4.2. In the analysis we assume quasi-uniformity of the triangulations, hence, $h \sim h_T := \mathrm{diam}(T)$, $T \in \mathcal{T}_h$. In the remainder we take a fixed Ω_h^{lin} with corresponding triangulation $\mathcal{T}_h$ and, to simplify the presentation, drop the index h.

The standard finite element space of continuous piecewise polynomials up to degree k with respect to the domain Ω^{lin} is denoted by V_h^k:

$$V_h^k := \{\, v_h \in C(\Omega^{\mathrm{lin}}) \mid v_{h|T} \in \mathcal{P}_k \quad \text{for all } T \in \mathcal{T}, \quad v_{h|\partial\Omega^{\mathrm{lin}}} = 0 \,\}.$$

The nodal interpolation operator in V_h^k is denoted by I_k. In the remainder we take a fixed $k \geq 1$. We are particularly interested in $k \geq 2$. This k denotes the polynomial degree of the finite element functions used in our finite element method (explained

in Section 4.4). To obtain a high order finite element discretization of (2.1) we need sufficiently accurate representations of $\partial\Omega$ and Γ. We now addresss these representations.

For simplicity we assume that all boundary vertices of $\partial\mathcal{T} = \partial\Omega^{\text{lin}}$ are located on $\partial\Omega$ (this assumption is not essential, cf. [4], Sect. 4.7). On $\partial\mathcal{T}$ we assume a given parametrization of the exact boundary $\partial\Omega$ of the form

$$g_b(x) = x + \chi_b(x), \tag{3.1}$$

such that $g_b : \partial\mathcal{T} \to \partial\Omega$ is a bijection. We assume that $\partial\Omega$ has smoothness properties such that the function χ_b can be chosen piecewise smooth on $\partial\mathcal{T}$ and satisfies

$$\|\chi_b\|_{\infty,\partial\mathcal{T}} + h\|D\chi_b\|_{\infty,\partial\mathcal{T}} \lesssim h^2 \text{ and } \max_{F\in\mathcal{F}(\partial\mathcal{T})} \|D^l\chi_b\|_{\infty,F} \lesssim 1,\ l = 2,..,k+1. \tag{3.2}$$

holds. Here $\mathcal{F}(\partial\mathcal{T})$ denotes the set of all boundary edges ($d = 2$) or boundary faces ($d = 3$). Note that $\chi_b(x_i) = 0$ at all boundary vertices x_i of $\partial\Omega^{\text{lin}}$. The function χ_b will be input for the parametric mapping used in our method.

We assume that the smooth interface Γ is the zero level of a smooth level set function $\phi : \Omega \to \mathbb{R}$, i.e., $\Gamma = \{\, x \in \Omega \mid \phi(x) = 0 \,\}$ and $\Omega_i = \{x \in \Omega \mid \phi(x) \lesseqgtr 0\}$. This level set function is not necessarily close to a distance function, but has the usual properties of a level set function:

$$\|\nabla\phi(x)\| \sim 1\ ,\ \ \|D^2\phi(x)\| \le c \quad \text{for all } x \ \text{ in a neighborhood } U \text{ of } \Gamma. \tag{3.3}$$

In the error analysis we assume that the level set function has the smoothness property $\phi \in C^{k+2}(U)$. As input for the parametric mapping we need an approximation $\phi_h \in V_h^k$ of ϕ, and we assume that this approximation satisfies the error estimate

$$\max_{T\in\mathcal{T}} |\phi_h - \phi|_{m,\infty,T\cap U} \lesssim h^{k+1-m}, \quad 0 \le m \le k+1. \tag{3.4}$$

Here $|\cdot|_{m,\infty,T\cap U}$ denotes the usual semi-norm on the Sobolev space $H^{m,\infty}(T \cap U)$ and the constant used in $\lesssim$ depends on ϕ but is independent of h. Note that (3.4) implies the estimate

$$\|\phi_h - \phi\|_{\infty,U} + h\|\nabla(\phi_h - \phi)\|_{\infty,U} \lesssim h^{k+1}. \tag{3.5}$$

The zero level of the finite element function ϕ_h (implicitly) characterizes the discrete interface. *The piecewise linear nodal interpolation of ϕ_h is denoted by $\hat{\phi}_h = I_1\phi_h$.* Hence, $\hat{\phi}_h(x_i) = \phi_h(x_i)$ at all vertices x_i in the triangulation $\mathcal{T}$. The low order geometry approximation of the interface, which is needed in our discretization method, is the zero level of this function:

$$\Gamma^{\text{lin}} := \{\hat{\phi}_h = 0\}.$$

The subdomains corresponding to Γ^{lin} are denoted by $\Omega_i^{\text{lin}} = \{x \in \Omega^{\text{lin}} \,|\, \hat{\phi}_h(x) \lesseqgtr 0\}$. Note that $\Omega_1^{\text{lin}} \cup \Omega_2^{\text{lin}} = \Omega^{\text{lin}} \neq \Omega$. All elements in the triangulation $\mathcal{T}$ which are cut by Γ^{lin} are collected in the set $\mathcal{T}^\Gamma := \{T \in \mathcal{T} \,|\, T \cap \Gamma^{\text{lin}} \neq \emptyset\}$. The corresponding domain is $\Omega^\Gamma := \{x \in T \,|\, T \in \mathcal{T}^\Gamma\}$.

We note that $\partial\Omega^{\text{lin}}$ and Γ^{lin} are (only) second order accurate approximations of $\partial\Omega$ and Γ, respectively. To achieve higher order accuracy with respect to the interface and the boundary approximation we consider a parametric mesh transformation in section 4.3.

4. Isoparametric mapping. The isoparametric mapping Θ_h, defined on $\Omega^{\rm lin}$, that is used in the finite element method is based on a *local* mapping Θ_h^Γ on Ω^Γ which is combined with a suitable *extension technique*. The latter is taken such that Θ_h^Γ is "smoothly" extended and Θ_h yields a sufficiently accurate boundary approximation. In the error analysis we need a mapping $\Psi : \Omega^{\rm lin} \to \Omega$ which is sufficiently close (in a higher order sense) to Θ_h and has the properties $\Psi(\Gamma^{\rm lin}) = \Gamma$, $\Psi(\partial\Omega^{\rm lin}) = \partial\Omega$. The construction of this Ψ is also based on a *local* mapping Ψ^Γ, that is very similar to Θ_h^Γ, which is extended with the same technique as used in the extension of Θ_h^Γ. The mappings Θ_h and Ψ for the case *without boundary approximation* (i.e., Ω is polygonal) are explained in detail in [24]. In the subsections below we explain how the construction of [24] can be extended to allow for isoparametric boundary approximation.

In section 4.1 we recall the definitions of the local mappings Θ_h^Γ, Ψ^Γ, which are the same as in [24]. In section 4.2 we discuss a general boundary data extension technique, which is essentially the same as the extension method used in isoparametric finite elements [25, 2]. In section 4.3 this extension technique is applied to both Θ_h^Γ and Ψ^Γ resulting in the global mappings Θ_h and Ψ. We give some results, e.g., on the smoothness of the extensions and on the approximation error in $\Theta_h \approx \Psi$, which are derived in [24]. These results are used in the error analysis.

4.1. Local mappings. In the construction of the local mapping Θ_h^Γ we need a projection step from a function which is piecewise polynomial but possibly discontinuous (across element interfaces) to the space of continuous finite element functions. Let $C(\mathcal{T}^\Gamma) := \bigoplus_{T\in\mathcal{T}^\Gamma} C(T)$ and $V_h^k(\Omega^\Gamma) := V_h^k|_{\Omega^\Gamma}$. We introduce a projection operator $P_h^\Gamma : C(\mathcal{T}^\Gamma)^d \to V_h^k(\Omega^\Gamma)^d$. The projection operator relies on a nodal representation of the finite element space $V_h^k(\Omega^\Gamma)$. The set of finite element nodes x_i in $\mathcal{T}^\Gamma$ is denoted by $\mathcal{N}(\mathcal{T}^\Gamma)$, and $\mathcal{N}(T)$ denotes the set of finite element nodes associated to $T \in \mathcal{T}^\Gamma$. All elements $T \in \mathcal{T}^\Gamma$ which contain the same finite element node x_i form the set denoted by $\omega(x_i) := \{\, T \in \mathcal{T}^\Gamma \mid x_i \in \mathcal{N}(T)\,\}$, $\quad x_i \in \mathcal{N}(\mathcal{T}^\Gamma)$. Let $|\cdot|$ denote the cardinality of the set $\omega(x_i)$ and let ψ_i be the nodal basis function corresponding to x_i. We define the projection operator $P_h^\Gamma : C(\mathcal{T}^\Gamma)^d \to V_h^k(\Omega^\Gamma)^d$ as

$$P_h^\Gamma v := \sum_{x_i\in\mathcal{N}(\mathcal{T}^\Gamma)} A_{x_i}(v)\,\psi_i, \text{ with } A_{x_i}(v) := \frac{1}{|\omega(x_i)|}\sum_{T\in\omega(x_i)} v_{|T}(x_i), \quad x_i \in \mathcal{N}(\mathcal{T}^\Gamma). \tag{4.1}$$

This is a simple and well-known projection operator considered also in e.g., [28, Eqs.(25)-(26)] and [11].

The construction of Θ_h^Γ is motivated by the following mapping $\Psi^\Gamma \in C(\Omega^\Gamma)$, defined in (4.3) below. We introduce the search direction $G := \nabla\phi$ and a function $d : \Omega^\Gamma \to \mathbb{R}$ defined as follows: $d(x)$ is the (in absolute value) smallest number such that

$$\phi(x + d(x)G(x)) = \hat{\phi}_h(x) \quad \text{for} \quad x \in \Omega^\Gamma. \tag{4.2}$$

(Recall that $\hat{\phi}_h$ is the piecewise linear nodal interpolation of ϕ_h.) Given the function $dG \in C(\Omega^\Gamma)^d \cap H^{1,\infty}(\Omega^\Gamma)^d$ we define:

$$\Psi^\Gamma(x) := x + d(x)G(x), \quad x \in \Omega^\Gamma. \tag{4.3}$$

Note that the function d and mapping Ψ^Γ depend on h, through $\hat{\phi}_h$ in (4.2). We do not show this dependence in our notation. By construction the mapping Ψ^Γ has the

property $\Psi^\Gamma(\Gamma^{\rm lin}) = \Gamma$. Further properties of Ψ^Γ are derived in [24, Corollary 3.2 and Lemma 3.4] and given in the following lemma.

LEMMA 4.1. *The following holds:*

$$|d(x_i)| \lesssim h^{k+1} \quad \textit{for all } \text{vertices } x_i \textit{ of } T \in \mathcal{T}^\Gamma, \tag{4.4a}$$

$$\|\Psi^\Gamma - \mathrm{id}\|_{\infty,\Omega^\Gamma} + h\|D\Psi^\Gamma - I\|_{\infty,\Omega^\Gamma} \lesssim h^2, \tag{4.4b}$$

$$\max_{T\in\mathcal{T}^\Gamma} \|D^l\Psi^\Gamma\|_{\infty,T} \lesssim 1, \quad l \le k+1. \tag{4.4c}$$

The mapping Ψ^Γ will be used in the error analysis, cf. section 4.3.

We now explain the construction of Θ_h^Γ, which consists of two steps. In the first step we introduce a discrete analogon of Ψ^Γ defined in (4.3), denoted by Ψ_h^Γ. Based on this Ψ_h^Γ, which can be discontinuous across element interfaces, we obtain a continuous transformation $\Theta_h^\Gamma \in C(\Omega^\Gamma)^d$ by averaging with the projection operator P_h^Γ. For the construction of Ψ_h^Γ we need an efficiently computable and accurate approximation of $G = \nabla\phi$ on $\mathcal{T}^\Gamma$. For this we consider the following two options

$$G_h(x) = \nabla\phi_h(x), \quad \text{or} \quad G_h(x) = (P_h^\Gamma \nabla\phi_h)(x), \quad x \in T \in \mathcal{T}^\Gamma. \tag{4.5}$$

Let $\mathcal{E}_T\phi_h$ be the polynomial extension of $\phi_h|_T$. We define a function $d_h : \mathcal{T}^\Gamma \to [-\delta, \delta]$, with $\delta > 0$ sufficiently small, as follows: $d_h(x)$ is the (in absolute value) smallest number such that

$$\mathcal{E}_T\phi_h(x + d_h(x)G_h(x)) = \hat{\phi}_h(x), \quad \text{for} \quad x \in T \in \mathcal{T}^\Gamma. \tag{4.6}$$

Clearly, this $d_h(x)$ is a "reasonable" approximation of the steplength $d(x)$ defined in (4.2). Given the function $d_hG_h \in C(\mathcal{T}^\Gamma)^d$ we define

$$\Psi_h^\Gamma(x) := x + d_h(x)G_h(x) \quad \text{for } x \in T \in \mathcal{T}^\Gamma, \tag{4.7}$$

which approximates the function Ψ^Γ defined in (4.3). To remove possible discontinuities of Ψ_h^Γ in Ω^Γ we apply the projection to obtain

$$\Theta_h^\Gamma := P_h^\Gamma\Psi_h^\Gamma = \mathrm{id} + P_h^\Gamma(d_hG_h). \tag{4.8}$$

The approximation result in the following lemma is from Lemma 3.6 in [24].

LEMMA 4.2. *The estimate*

$$\sum_{r=0}^{k+1} h^r \max_{T\in\mathcal{T}^\Gamma} \|D^r(\Theta_h^\Gamma - \Psi^\Gamma)\|_{\infty,T} \lesssim h^{k+1} \tag{4.9}$$

holds.

4.2. Finite element boundary data extension method. Let $\hat{\mathcal{T}} \subset \mathcal{T}$ be a subset of the triangulation such that $\hat{\Omega}^{\rm lin} := \cup_{T\in\hat{\mathcal{T}}} T$ is a connected subdomain of $\Omega^{\rm lin}$. We also need the notation $\partial\hat{\mathcal{T}} = \partial\hat{\Omega}^{\rm lin}$, $\hat{\mathcal{T}}^{\rm bnd} := \{T \in \hat{\mathcal{T}} \mid T \cap \partial\hat{\mathcal{T}} \neq \emptyset\}$, $\hat{\mathcal{T}}^{\rm int} = \hat{\mathcal{T}} \setminus \hat{\mathcal{T}}^{\rm bnd}$, cf. Figure 4.1 (left). Given such a connected triangulation $\hat{\mathcal{T}}$, boundary data $g \in C(\partial\hat{\Omega}^{\rm lin})$ and a polynomial degree $k \ge 1$, a *linear extension operator* $\mathcal{E}_k(\hat{\mathcal{T}}, g)$ is treated in [24], which is essentially the same as the finite element extension technique studied in [25, 2]. This type of extension operator is a standard component in isoparametric finite element methods for high order boundary approximations.

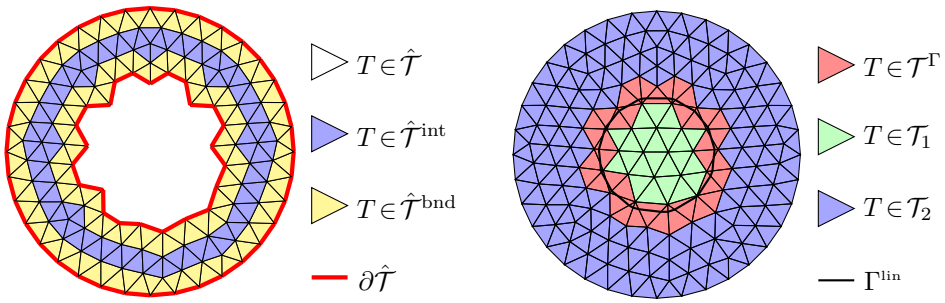

FIG. 4.1. *Connected subtriangulation $\hat{\mathcal{T}} \subset \mathcal{T}$ with $\hat{\mathcal{T}}^{\text{int}}$, $\hat{\mathcal{T}}^{\text{bnd}}$ and $\partial\hat{\mathcal{T}}$ (left) and decomposition of a triangulation $\mathcal{T}$ into $\mathcal{T}^{\Gamma}$, $\mathcal{T}_1$ and $\mathcal{T}_2$ (right).*

This operator is local, meaning that it is applied elementwise for $T \in \hat{\mathcal{T}}^{\text{bnd}}$. Its construction is hierarchical in the sense that first an extension based on values at vertices lying on $\partial\hat{\mathcal{T}}$ is determined, then an extension from edges lying on $\partial\hat{\mathcal{T}}$ and finally (for the three-dimensional case) an extension of the data from faces lying on $\partial\hat{\mathcal{T}}$ is determined. For a precise definition of this operator we refer to [24]. In the following lemma we summarize some properties of this operator which are derived in [24, 25, 2].

LEMMA 4.3. *Let $\mathcal{V}(\partial\hat{\mathcal{T}})$ denote the set of vertices in $\partial\hat{\mathcal{T}}$ and $\mathcal{F}(\partial\hat{\mathcal{T}})$ the set of all edges ($d = 2$) or faces ($d = 3$) in $\partial\hat{\mathcal{T}}$. For $\mathcal{E}(g) := \mathcal{E}_k(\hat{\mathcal{T}}, g)$ the following holds*

$$\mathcal{E}(g) \in C(\hat{\Omega}^{lin}), \quad \mathcal{E}(g) = 0 \quad \text{on } \hat{T}^{\text{int}}, \quad \mathcal{E}(g)_{|\partial\hat{\mathcal{T}}} = g. \tag{4.10a}$$

$$\text{For all } T \in \hat{\mathcal{T}}^{\text{bnd}} : \quad \text{if } T \cap \partial\hat{\mathcal{T}} \in \mathcal{V}(\partial\hat{\mathcal{T}}) \text{ then } \mathcal{E}(g) \in \mathcal{P}_1(T). \tag{4.10b}$$

$$\text{For all } T \in \hat{\mathcal{T}}^{\text{bnd}} : \quad \text{if } g \in \mathcal{P}_k(T \cap \partial\hat{\mathcal{T}}) \text{ then } \mathcal{E}(g) \in \mathcal{P}_k(T). \tag{4.10c}$$

Furthermore,

$$\begin{aligned} \|D^n \mathcal{E}(g)\|_{\infty,\hat{\Omega}^{lin}} \lesssim & \max_{F \in \mathcal{F}(\partial\hat{\mathcal{T}})} \sum_{r=n}^{k+1} h^{r-n} \|D^r g\|_{\infty,F} \\ & + h^{-n} \max_{x_i \in \mathcal{V}(\partial\hat{\mathcal{T}})} |g(x_i)|, \quad n = 0, 1, \end{aligned} \tag{4.10d}$$

$$\max_{T \in \hat{\mathcal{T}}} \|D^n \mathcal{E}(g)\|_{\infty,T} \lesssim \sum_{r=n}^{k+1} h^{r-n} \|D^r g\|_{\infty,F}, \quad n = 2, \ldots, k+1, \tag{4.10e}$$

for all $g \in C(\partial\hat{T})$ such that $g \in C^{k+1}(F)$ for all $F \in \mathcal{F}(\partial\hat{\mathcal{T}})$.

The results in (4.10a)-(4.10c) give basic structural properties of the extension operator. In particular the result in (4.10c) yields that piecewise polynomial boundary data result in piecewise polynomial extensions of the same degree. The results in (4.10d), (4.10e) measure smoothness properties of the extension in terms of the smoothness of the boundary data.

4.3. Global isoparametric mapping. We use the local mappings Θ_h^{Γ}, Ψ^{Γ} on Ω^{Γ} and the boundary parametrization χ_b as in (3.1), and combine these with the extension technique to obtain global mappings Θ_h and Ψ. For this we decompose the triangulation $\mathcal{T}$ into disjoint subsets as follows

$$\mathcal{T} = \mathcal{T}^{\Gamma} \cup \mathcal{T}_1 \cup \mathcal{T}_2, \quad \text{with } \mathcal{T}_1 := \{\, T \in \mathcal{T} \mid (\hat{\phi}_h)_{|T} < 0 \,\}, \ \ \mathcal{T}_2 := \{\, T \in \mathcal{T} \mid (\hat{\phi}_h)_{|T} > 0 \,\}.$$

We assumed that $\overline{\Omega}_1$ (where $\phi < 0$ holds) is strictly contained in Ω. Hence (for h sufficiently small) we have that $\mathcal{T}_1$ is strictly contained in Ω. On $\partial\mathcal{T}_1$ we have boundary data Θ_h and Ψ^Γ, which will be extended to $\mathcal{T}_1$, cf. below. The boundary of $\mathcal{T}_2$ consists of two disjoint parts, namely $\partial\mathcal{T}_2 = \partial\mathcal{T} \cup (\partial\mathcal{T}_2 \setminus \partial\mathcal{T})$, cf. Figure 4.1 (right). On $(\partial\mathcal{T}_2 \setminus \partial\mathcal{T}) \subset \partial\mathcal{T}^\Gamma$ we have boundary data Θ_h and Ψ^Γ. On $\partial\mathcal{T}$ we have boundary data given by the parametrization χ_b. Below, boundary data on the two parts $\partial\mathcal{T}_2 \setminus \partial\mathcal{T}$ and $\partial\mathcal{T}$ of $\partial\mathcal{T}_2$ are denoted as a pair of functions (g_1, g_2). Using the extension technique, the local mappings Ψ^Γ and Θ_h^Γ on Ω^Γ we can define *global* mappings Ψ, Θ_h as follows:

$$\Psi := \begin{cases} \Psi^\Gamma & \text{on} \quad \mathcal{T}^\Gamma, \\ \mathrm{id} + \mathcal{E}_k\big(\mathcal{T}_1, (\Psi^\Gamma - \mathrm{id})\big) & \text{on} \quad \mathcal{T}_1, \\ \mathrm{id} + \mathcal{E}_k\big(\mathcal{T}_2, (\Psi^\Gamma - \mathrm{id}, \quad \chi_b)\big) & \text{on} \quad \mathcal{T}_2, \end{cases} \tag{4.11a}$$

$$\Theta_h := \begin{cases} \Theta_h^\Gamma & \text{on} \quad \mathcal{T}^\Gamma, \\ \mathrm{id} + \mathcal{E}_k\big(\mathcal{T}_1, (\Theta_h^\Gamma - \mathrm{id})\big) & \text{on} \quad \mathcal{T}_1, \\ \mathrm{id} + \mathcal{E}_k\big(\mathcal{T}_2, (\Theta_h^\Gamma - \mathrm{id}, I_k\chi_b)\big) & \text{on} \quad \mathcal{T}_2. \end{cases} \tag{4.11b}$$

Here $I_k\chi_b$ denotes the piecewise polynomial nodal interpolation of the boundary parametrization χ_b on the edges ($d = 2$) or faces ($d = 3$) that are on $\partial\mathcal{T}$.

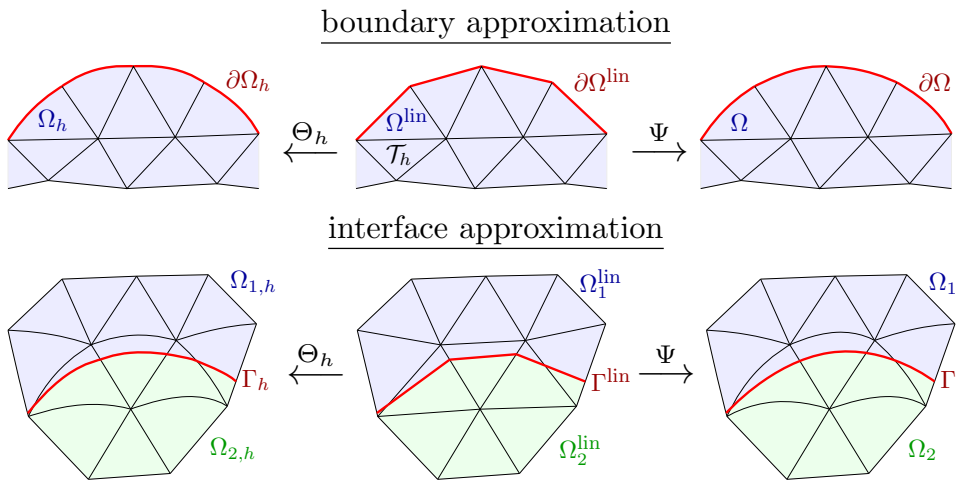

FIG. 4.2. *Sketch of geometries. The basis is the polygonal approximation (center) of the boundary (top row) and the interface (bottom row). The parametric mapping Θ_h (left) is used in the discretization method and essential for the higher order accuracy. The mapping Ψ (right) maps the discrete boundary and interface approximations to the exact geometries and is used in the error analysis below.*

4.4. Isoparametric unfitted finite element method. We introduce the isoparametric unfitted finite element method, based on the isoparametric mapping Θ_h, for the discretization of the model elliptic interface problem (2.1). We define the isoparametric Nitsche unfitted FEM as a transformed version of the original Nitsche unfitted FE discretization [17] with respect to the interface approximation $\Gamma_h = \Theta_h(\Gamma^{\mathrm{lin}})$. We introduce some further notation. The standard unfitted space w.r.t. Γ^{lin} is denoted by

$$V_h^\Gamma := V_{h\,|\Omega_{h,1}^{\mathrm{lin}}}^k \oplus V_{h\,|\Omega_{h,2}^{\mathrm{lin}}}^k.$$

To simplify the notation we do not explicitly express the polynomial degree k in V_h^Γ. The *isoparametric unfitted FE space* is defined as

$$V_{h,\Theta}^\Gamma := \{\, v_h \circ \Theta_h^{-1} \mid v_h \in V_h^\Gamma \,\} = \{\, \tilde{v}_h \mid \tilde{v}_h \circ \Theta_h \in V_h^\Gamma \,\}. \tag{4.12}$$

Note that functions from $V_{h,\Theta}^\Gamma$ are defined on the isoparametrically transformed domain $\Omega_h = \Omega_{1,h} \cup \Omega_{2,h}$, with $\Omega_{i,h} := \Theta_h(\Omega_i^{\text{lin}})$. Based on this space we formulate a discretization of (2.1) using the Nitsche technique [17] with $\Omega_{i,h}$, $i = 1, 2$, as numerical approximation of the subdomains Ω_i: determine $u_h \in V_{h,\Theta}^\Gamma$ such that

$$A_h(u_h, v_h) := a_h(u_h, v_h) + N_h(u_h, v_h) = f_h(v_h) \quad \text{for all } v_h \in V_{h,\Theta}^\Gamma, \tag{4.13}$$

with the bilinear and linear forms

$$a_h(u, v) := \sum_{i=1}^{2} \alpha_i \int_{\Omega_{i,h}} \nabla u \cdot \nabla v \; dx, \tag{4.14a}$$

$$N_h(u, v) := N_h^c(u, v) + N_h^c(v, u) + N_h^s(u, v), \tag{4.14b}$$

$$N_h^c(u, v) := \int_{\Gamma_h} \{\!\{-\alpha \nabla v\}\!\} \cdot n [\![u]\!] \; ds, \quad N_h^s(u, v) := \bar{\alpha} \frac{\lambda}{h} \int_{\Gamma_h} [\![u]\!][\![v]\!] \; ds, \tag{4.14c}$$

for $u, v \in V_{h,\Theta}^\Gamma + V_{\text{reg},h}$ with $V_{\text{reg},h} := H^1(\Omega_h) \cap (H^2(\Omega_{1,h}) \cup H^2(\Omega_{2,h}))$. Furthermore, $n = n_{\Gamma_h}$ denotes the outer normal on the boundary Γ_h of $\Omega_{1,h}$ and $\bar{\alpha} = \frac{1}{2}(\alpha_1 + \alpha_2)$ the mean diffusion coefficient. For the averaging operator $\{\!\{\cdot\}\!\}$ there are different possibilities. We use $\{\!\{w\}\!\} := \kappa_1 w_{|\Omega_{1,h}} + \kappa_2 w_{|\Omega_{2,h}}$ with a "Heaviside" choice where $\kappa_1 + \kappa_2 = 1$ with $\kappa_1 = 1$ if $|T_1| > \frac{1}{2}|T|$ and $\kappa_1 = 0$ otherwise. Here, $T_i = T \cap \Omega_i^{\text{lin}}$, i.e. the cut configuration on the undeformed mesh is used. This choice in the averaging renders the scheme in (4.13) stable (for sufficiently large λ) for arbitrary polynomial degrees k, independent of the cut position of Γ (Lemma 5.2 in [24]). A different choice for the averaging which also results in a stable scheme is $\kappa_i = |T_i|/|T|$.

In order to define the right hand side functional f_h we first assume that the source term $f_i : \Omega_i \to \mathbb{R}$ in (2.1a) is (smoothly) extended to $\Omega_{i,h}$. This extension is denoted by $f_{i,h}$ and satisfies $f_{i,h} = f_i$ on Ω_i. We define f_h on Ω by $f_{h|\Omega_{i,h}} := f_{i,h}$, $i = 1, 2$, hence,

$$f_h(v) := \int_{\Omega_h} f_h v \, dx = \sum_{i=1,2} \int_{\Omega_{i,h}} f_{i,h} v dx. \tag{4.15}$$

Remark 1. For the implementation of this method we use the same technique as in standard isoparametric finite element methods. In the integrals we apply a transformation of variables $y := \Theta_h^{-1}(x)$. For example, the bilinear form $a_h(u, v)$ then results in

$$a_h(u, v) := \sum_{i=1,2} \alpha_i \int_{\Omega_i^{\text{lin}}} D\Theta_h^{-T} \nabla u \cdot D\Theta_h^{-T} \nabla v \;\; \det(D\Theta_h) \, dy. \tag{4.16}$$

Based on this transformation the implementation of integrals is carried out as for the case of the piecewise planar interface Γ^{lin}. The additional variable coefficients $D\Theta_h^{-T}$, $\det(D\Theta_h)$ are easily and efficiently computable using the property that Θ_h is a finite element (vector) function.

5. Preliminaries for the error analysis. In this section we collect results from [24] that we need in the proof of the L^2-estimate in Section 6. In [24] the case *without* an isoparametric boundary approximation is considered. It turns out that the results that we need from [24] also hold for the case with isoparametric boundary approximation, i.e., with the mapping Θ_h in (4.11b), and that the proofs given in [24] require only minor modifications. In the proofs below we refer to the analysis given in [24] and explain only the modifications needed due to the additional isoparametric boundary approximation.

In the error analysis we use the norm

$$\|v\|_h^2 := |v|_1^2 + \|[\![v]\!]\|_{\frac{1}{2},h,\Gamma_h}^2 + \|\{\!\{\alpha\nabla v\}\!\}\|_{-\frac{1}{2},h,\Gamma_h}^2, \tag{5.1}$$

$$\text{with } \|v\|_{\pm\frac{1}{2},h,\Gamma_h}^2 := (\bar{\alpha}/h)^{\pm 1}\,\|v\|_{L^2(\Gamma_h)}^2 \text{ and } |v|_1^2 := \sum_{i=1,2}\alpha_i\|\nabla v\|_{L^2(\Omega_{i,h})}^2. \tag{5.2}$$

Note that the norms are formulated with respect to $\Omega_{i,h} = \Theta_h(\Omega_i^{\text{lin}})$ and $\Gamma_h = \Theta_h(\Gamma^{\text{lin}})$ and include a scaling depending on α. The norm $\|\cdot\|_h$ and the bilinear forms in (4.14) are well-defined on $V_{h,\Theta}^{\Gamma} + V_{\text{reg},h}$.

LEMMA 5.1 (Ellipticity and continuity). *For λ sufficiently large the estimates*

$$A_h(u,u) \gtrsim \|u\|_h^2 \qquad \textit{for all } u \in V_{h,\Theta}^{\Gamma}, \tag{5.3a}$$

$$A_h(u,v) \lesssim \|u\|_h\|v\|_h \qquad \textit{for all } u,v \in V_{h,\Theta}^{\Gamma} + V_{reg,h} \tag{5.3b}$$

hold.

Proof. The proof given in [24, Lemma 5.2] applies without any modifications. We note that a crucial component in the proof is the assessment that L^2 and H^1 norms on $\Omega_{i,h}$ and Γ_h are equivalent to corresponding norms of mapped functions on Ω_i^{lin} and Γ^{lin}, cf. [24, Lemma 3.12]. Due to this the ellipticity and continuity can equivalently be shown on a piecewise linear interface approximation with Γ^{lin}. □

In the remainder we assume that λ is taken sufficiently large such that the results in Lemma 5.1 hold. Then the discrete problem (4.13) has a unique solution.

A key component of the error analysis in [24] is the mapping $\Phi_h := \Psi \circ \Theta_h^{-1}$. For the derivation of properties of this mapping we first derive useful results for Ψ.

THEOREM 5.2. *For Ψ the following holds:*

$$\|\Psi - \text{id}\|_{\infty,\Omega} + h\|D\Psi - I\|_{\infty,\Omega} \lesssim h^2, \tag{5.4}$$

$$\max_{T\in\mathcal{T}}\|D^l\Psi\|_{\infty,T} \lesssim 1, \quad 0 \le l \le k+1. \tag{5.5}$$

Proof. On $\mathcal{T}^{\Gamma}$ the results are a direct consequence of Lemma 4.1. On $\mathcal{T}_1 \cup \mathcal{T}_2$ the result in (5.5) for $l = 0,1$ follows from (5.4) and for $l \ge 2$ it follows from (4.10e) combined with (4.4c) and (3.2). It remains to derive the estimate as in (5.4) on $\mathcal{T}_1 \cup \mathcal{T}_2$. We consider $\mathcal{T}_2$ and write $\mathcal{E}(\Psi^{\Gamma} - \text{id}, \chi_b) := \mathcal{E}_k\big(\mathcal{T}_2, (\Psi^{\Gamma} - \text{id}, \chi_b)\big)$. Using (4.10d) and

$\chi_b(x_i) = 0$ at vertices $x_i \in \partial\mathcal{T}$ we get

$$
\begin{aligned}
&\|\Psi - \mathrm{id}\|_{\infty,\mathcal{T}_2} + h\|D\Psi - I\|_{\infty,\mathcal{T}_2} \\
&\qquad = \|\mathcal{E}(\Psi^\Gamma - \mathrm{id}, \chi_b)\|_{\infty,\mathcal{T}_2} + h\|D\mathcal{E}(\Psi^\Gamma - \mathrm{id}, \chi_b)\|_{\infty,\mathcal{T}_2} \\
&\qquad \overset{(4.10d)}{\lesssim} \sum_{r=0}^{k+1} h^r \Big(\max_{F\in\mathcal{F}(\partial\mathcal{T}_2\setminus\partial\mathcal{T})} \|D^r(\Psi^\Gamma - \mathrm{id})\|_{\infty,F} + \max_{F\in\mathcal{F}(\partial\mathcal{T})} \|D^r\chi_b\|_{\infty,F} \Big) \\
&\qquad\quad + \max_{x_i\in\mathcal{V}(\partial\mathcal{T}_2\setminus\partial\mathcal{T})} |(\Psi^\Gamma - \mathrm{id})(x_i)| \\
&\qquad \lesssim \underbrace{\|\Psi^\Gamma - \mathrm{id}\|_{\infty,\mathcal{T}^\Gamma} + h\|D\Psi^\Gamma - I\|_{\infty,\mathcal{T}^\Gamma}}_{\lesssim h^2 \quad \text{(Lemma 4.1)}} + h^2 \underbrace{\max_{2\le l\le k+1} \max_{T\in\mathcal{T}^\Gamma} \|D^l\Psi^\Gamma\|_{\infty,T}}_{\lesssim 1 \quad \text{(Lemma 4.1)}} \\
&\qquad\quad + \underbrace{\sum_{r=0}^{k+1} h^r \max_{F\in\mathcal{F}(\partial\mathcal{T})} \|D^r\chi_b\|_{\infty,F}}_{\lesssim h^2 \quad (3.2)} + \underbrace{\max_{x_i\in\mathcal{V}(\mathcal{T}^\Gamma)} |d(x_i)|}_{\lesssim h^2 \quad \text{(Lemma 4.1)}} \lesssim h^2.
\end{aligned}
$$

For $\mathcal{T}_1$ similar arguments can be applied. □

The proof above generalizes the one given in [24] since it allows a boundary approximation via the function $g_b(x) = x + \chi_b(x)$.

From (5.4) it follows that, for h sufficiently small, Ψ is a bijection on Ω. Furthermore this mapping induces a family of (curved) finite elements that is regular of order k, in the sense as defined in [2]. The corresponding curved finite element space is given by

$$
V_{h,\Psi} := \{\, v_h \circ \Psi_h^{-1} \mid v_h \in V_h^k \,\}. \tag{5.6}
$$

Due to the results in Theorem 5.2 the analysis of the approximation error for this finite element space as developed in [2] can be applied. Corollary 4.1 from that paper yields that there exists an interpolation operator $\Pi_h : H^{k+1}(\Omega) \to V_{h,\Psi}$ such that

$$
\|u - \Pi_h u\|_{L^2(\Omega)} + h\|u - \Pi_h u\|_{H^1(\Omega)} \lesssim h^{k+1}\|u\|_{H^{k+1}(\Omega)} \quad \text{for all } u \in H^{k+1}(\Omega). \tag{5.7}
$$

For h sufficiently small, the mapping $\Phi_h = \Psi \circ \Theta_h^{-1} : \Omega_h \to \Omega$ is a bijection and has the property $\Phi_h(\Gamma_h) = \Gamma$, cf. Fig. 4.2. In the remainder we assume that h is sufficiently small such that Φ_h is a bijection. It has the smoothness property $\Phi_h \in C(\Omega_h)^d \cap C^{k+1}(\Theta_h(\mathcal{T}))^d$. In the following lemma we derive further properties of Φ_h that will be needed in the error analysis.

Lemma 5.3. *The following holds:*

$$
\|\Theta_h - \Psi\|_{\infty,\Omega^{lin}} + h\|D(\Theta_h - \Psi)\|_{\infty,\Omega^{lin}} \lesssim h^{k+1}, \tag{5.8}
$$

$$
\|\Phi_h - \mathrm{id}\|_{\infty,\Omega^{lin}} + h\|D\Phi_h - I\|_{\infty,\Omega^{lin}} \lesssim h^{k+1}. \tag{5.9}
$$

Proof. The estimate (5.8) follows by using the linearity of the extension operator $\mathcal{E}_k$, cf. (4.11), and then using argmuments very similar to the ones used in the proof of Theorem 5.2. Note that $\Phi_h - \mathrm{id} = (\Psi - \Theta_h)\Theta_h^{-1}$. From the results in (5.4) and (5.8) it follows that $\|\Theta_h^{-1}\|_{\infty,\Omega_h} \lesssim 1$, $\|D\Theta_h^{-1}\|_{\infty,\Omega_h} \lesssim 1$. Hence, the estimate in (5.9) follows from the one in (5.8). □

We define $V_{\text{reg}} := H^1(\Omega) \cap H^2(\Omega_1 \cup \Omega_2)$. Related to Φ_h we define the following transformed unfitted finite element space, cf. (4.12),

$$V_{h,\Phi}^{\Gamma} := \{v \circ \Phi_h^{-1}, v \in V_{h,\Theta}^{\Gamma}\} \subset H^1(\Omega_1 \cup \Omega_2),$$

and the linear and bilinear forms

$$A(u,v) := a(u,v) + N(u,v), \quad f(v) = \int_\Omega f v \, dx, \quad u, v \in V_{h,\Phi}^{\Gamma} + V_{\text{reg}}, \tag{5.10}$$

with the bilinear forms $a(\cdot,\cdot)$, $N(\cdot,\cdot)$ as in (4.14) with $\Omega_{i,h}$ and Γ_h replaced with Ω_i and Γ, respectively. In the following lemma a consistency result is given.

LEMMA 5.4 (Consistency). *Let $u \in V_{reg}$ be a solution of* (2.1). *The following holds:*

$$A(u,v) = f(v) \quad \textit{for all } \ v \in V_{h,\Phi}^{\Gamma} + V_{reg}. \tag{5.11}$$

Proof. Proof is given in [24]. No modifications are needed. □

We introduce the subdomain

$$U_\delta := \{\, x \in \Omega \mid \operatorname{dist}(x,\Gamma) \le \delta \text{ or } \operatorname{dist}(x,\partial\Omega) \le \delta \,\},$$

with $\delta > 0$ (sufficiently small), consisting of a tubular neigborhood of the interface Γ and a strip adjacent to $\partial\Omega$. To bound the consistency errors with respect to A_h we use the following result.

LEMMA 5.5. *For $\delta > 0$ sufficiently small and $u \in H^1(\Omega_1 \cup \Omega_2)$ there holds*

$$\|u\|_{L^2(U_\delta)} \le c\delta^{\frac{1}{2}} \|u\|_{H^1(\Omega_1 \cup \Omega_2)}. \tag{5.12}$$

Proof. See [10, Lemma 4.10]. □

With this result a consistency bound from [24] can be improved.

LEMMA 5.6 (Consistency bounds). *Let $u \in V_{reg}$ be a solution of* (2.1). *We assume $f \in H^{1,\infty}(\Omega_1 \cup \Omega_2)$ and a data extension f_h, used in* (4.15), *that satisfies $\|f_h\|_{H^{1,\infty}(\Omega_{1,h} \cup \Omega_{2,h})} \lesssim \|f\|_{H^{1,\infty}(\Omega_1 \cup \Omega_2)}$. The following estimates hold for $w_h \in V_{h,\Theta}^{\Gamma} + V_{reg,h}$:*

$$|A(u, w_h \circ \Phi_h^{-1}) - A_h(u \circ \Phi_h, w_h)| \lesssim h^k \|u\|_{H^2(\Omega_1 \cup \Omega_2)} \|w_h\|_h, \tag{5.13a}$$

$$|f(w_h \circ \Phi_h^{-1}) - f_h(w_h)| \lesssim h^{k+1} \|f\|_{H^{1,\infty}(\Omega_1 \cup \Omega_2)} \|w_h\|_h. \tag{5.13b}$$

Proof. In [24, Lemma 5.13] equation (5.13a) is derived for the case without isoparametric boundary approximation. The proof applies, without modifications, also to the case with isoparametric boundary approximation. In [24, Lemma 5.13] a bound as in (5.13b) with h^{k+1} replaced by h^k is derived. We now show how one obtains the improved bound in (5.13b). Define $\Delta_h := U_{\delta_h}$, which $\delta_h := ch$ and $c > 0$ sufficiently large such that $\Phi_h^{-1} \neq \text{id}$ only on Δ_h. Note that

$$\begin{aligned} |f(w_h \circ \Phi_h^{-1}) - f_h(w_h)| &= \left| \int_\Omega f(w_h \circ \Phi_h^{-1}) \, dx - \int_{\Omega_h} f_h w_h \, dx \right| \\ &\le \sum_{i=1}^{2} \left| \int_{\Omega_i} f_i (w_h \circ \Phi_h^{-1}) \, dx - \int_{\Omega_{i,h}} f_{i,h} w_h \, dx \right|. \end{aligned}$$

For $i = 1, 2$ and using $f_{i,h} = f_i$ on Ω_i we get:

$$\left| \int_{\Omega_i} f_i (w_h \circ \Phi_h^{-1})\, dx - \int_{\Omega_{i,h}} f_{i,h} w_h \, dx \right| = \left| \int_{\Omega_{i,h}} \big(\det(D\Phi_h)(f_{i,h} \circ \Phi_h) - f_{i,h} \big) w_h \, dx \right|$$
$$\leq \int_{\Delta_h \cap \Omega_{i,h}} |(\det(D\Phi_h) - I) f_{i,h} w_h| \, dx + \int_{\Delta_h \cap \Omega_{i,h}} |\det(D\Phi_h)((f_{i,h} \circ \Phi_h) - f_{i,h}) w_h| \, dx$$
$$\leq |\Delta_h|^{\frac{1}{2}} \, \| \det(D\Phi_h) - I \|_{\infty,\Omega_h} \|f_h\|_{\infty,\Omega_h} \|w_h\|_{L^2(\Delta_h)}$$
$$+ |\Delta_h|^{\frac{1}{2}} \, \| \det(D\Phi_h) \|_{\infty,\Omega_h} \|f_h\|_{H^{1,\infty}(\Omega_{1,h} \cup \Omega_{2,h})} \|\Phi_h - \mathrm{id}\|_{\infty,\Omega_h} \|w_h\|_{L^2(\Delta_h)}$$
$$\lesssim h^{k+\frac{1}{2}} \|f\|_{H^{1,\infty}(\Omega_{1,h} \cup \Omega_{2,h})} \|w_h\|_{L^2(\Delta_h)}.$$

In the last inequality we used the properties of the transformation Φ_h from (5.9). Next, we apply Lemma 5.5 to gain another factor $h^{\frac{1}{2}}$:

$$\begin{aligned} \|w_h\|_{L^2(\Delta_h)} &\lesssim \|w_h \circ \Phi_h^{-1}\|_{L^2(\Phi_h(\Delta_h))} \leq \|w_h \circ \Phi_h^{-1}\|_{L^2(U_{\delta_h})} \\ &\lesssim \delta_h^{\frac{1}{2}} \|w_h \circ \Phi_h^{-1}\|_{H^1(\Omega_1 \cup \Omega_2)} \lesssim h^{\frac{1}{2}} \|w_h\|_{H^1(\Omega_{1,h} \cup \Omega_{2,h})} \lesssim h^{\frac{1}{2}} \|w_h\|_h. \end{aligned} \tag{5.14}$$

Combining these results completes the proof. □

The main result of [24] is given in the following theorem.

THEOREM 5.7 (Discretization error bound). *Let u be the solution of* (2.1) *and $u_h \in V_{h,\Theta}^{\Gamma}$ the solution of* (4.13)*. We assume that $u \in H^{k+1}(\Omega_1 \cup \Omega_2)$ and the data extension f_h satisfies the condition in Lemma 5.6. Then the following holds:*

$$\|u \circ \Phi_h - u_h\|_h \lesssim h^k (\|u\|_{H^{k+1}(\Omega_1 \cup \Omega_2)} + \|f\|_{H^{1,\infty}(\Omega_1 \cup \Omega_2)}), \tag{5.15}$$
$$|u - u_h \circ \Phi_h^{-1}|_{H^1(\Omega_1 \cup \Omega_2)} \lesssim h^k (\|u\|_{H^{k+1}(\Omega_1 \cup \Omega_2)} + \|f\|_{H^{1,\infty}(\Omega_1 \cup \Omega_2)}). \tag{5.16}$$

Proof. The result (5.16) easily follows from (5.15) using the definition of the norm $\|\cdot\|_h$ and properties of Φ_h. The proof of (5.15) in [24] applies with only minor modifications. A key ingredient in the proof is the following approximation property, which holds for arbitrary $u \in H^{k+1}(\Omega_1 \cup \Omega_2)$:

$$\inf_{v_h \in V_{h,\Theta}^{\Gamma}} \|u \circ \Phi_h - v_h\|_h \lesssim h^k \|u\|_{H^{k+1}(\Omega_1 \cup \Omega_2)}, \tag{5.17}$$

which is based on the isoparametric interpolation error bound (5.7). □

6. L^2-error bound. In this section we present an L^2-norm discretization error bound for the unfitted finite element method in (4.13). The key ingredients are a duality argument, the already available H^1-error bound given in Theorem 5.7 and the consistency error bound (5.13a)-(5.13b).

In the remainder we assume that the smoothness conditions on the solution u and the right hand side f as formulated in Theorem 5.7 are satisfied. We define the discretization error $e_h := u - u_h \circ \Phi_h^{-1} \in H^1(\Omega_1 \cup \Omega_2)$ and consider the (adjoint) problem:

$$-\mathrm{div}(\alpha_i \nabla z) = e_h \quad \text{in } \Omega_i, \ i = 1, 2, \tag{6.1a}$$
$$[\![\alpha \nabla z]\!]_\Gamma \cdot n_\Gamma = 0, \quad [\![z]\!]_\Gamma = 0 \quad \text{on } \Gamma, \tag{6.1b}$$
$$z = 0 \quad \text{on } \partial\Omega. \tag{6.1c}$$

We assume that Γ and $\partial\Omega$ are sufficiently smooth such that the following regularity property holds:

$$\|z\|_{H^2(\Omega_1\cup\Omega_2)} \lesssim \|e_h\|_{L^2(\Omega)}, \tag{6.2}$$

cf. [18, 7, 20]. From Lemma 5.4 we obtain the identity $\|e_h\|^2_{L^2(\Omega)} = A(z, e_h)$. The L^2-error analysis is based on the following splitting, with $z_h \in V^\Gamma_{h,\Theta}$:

$$\begin{aligned}
\|e_h\|^2_{L^2(\Omega)} &= A(z, e_h) \\
&= A(z, e_h) - A_h(z\circ\Phi_h, e_h\circ\Phi_h) && \text{(6.3a)}\\
&\quad + A_h(z\circ\Phi_h - z_h, e_h\circ\Phi_h) && \text{(6.3b)}\\
&\quad + A_h(u\circ\Phi_h, z_h) - A(u, z_h\circ\Phi_h^{-1}) && \text{(6.3c)}\\
&\quad + f(z_h\circ\Phi_h^{-1}) - f_h(z_h). && \text{(6.3d)}
\end{aligned}$$

In the lemmas below we derive bounds for the terms in (6.3a)-(6.3d).

Lemma 6.1. *The estimate*

$$|A(z, e_h) - A_h(z\circ\Phi_h, e_h\circ\Phi_h)| \lesssim h^{2k}\big(\|u\|_{H^{k+1}(\Omega_1\cup\Omega_2)} + \|f\|_{H^{1,\infty}(\Omega_1\cup\Omega_2)}\big)\|e_h\|_{L^2(\Omega)}$$

holds.

Proof. Note that $e_h\circ\Phi_h \in V^\Gamma_{h,\Theta} + V_{\mathrm{reg},h}$. We use (5.13a) with $w_h = e_h\circ\Phi_h$, z instead of u and combine this with the regulariy estimate (6.2) and the result in Theorem 5.7. This yields

$$\begin{aligned}
|A(z, e_h) - A_h(z\circ\Phi_h, e_h\circ\Phi_h)| &\lesssim h^k\|z\|_{H^2(\Omega_1\cup\Omega_2)}\|e_h\circ\Phi_h\|_h \\
&\lesssim h^{2k}\big(\|u\|_{H^{k+1}(\Omega_1\cup\Omega_2)} + \|f\|_{H^{1,\infty}(\Omega_1\cup\Omega_2)}\big)\|e_h\|_{L^2(\Omega)},
\end{aligned}$$

which completes the proof. □

In the terms (6.3b)-(6.3d) we need a suitable $z_h \in V^\Gamma_{h,\Theta}$. For this we take $z_h \in V^\Gamma_{h,\Theta}$ such that the following holds, cf. (5.17):

$$\|z\circ\Phi_h - z_h\|_h \lesssim h\|z\|_{H^2(\Omega_1\cup\Omega_2)} \lesssim h\|e_h\|_{L^2(\Omega)}. \tag{6.4}$$

Lemma 6.2. *Let z_h be as in* (6.4). *The estimate*

$$|A_h(z\circ\Phi_h - z_h, e_h\circ\Phi_h)| \lesssim h^{k+1}\big(\|u\|_{H^{k+1}(\Omega_1\cup\Omega_2)} + \|f\|_{H^{1,\infty}(\Omega_1\cup\Omega_2)}\big)\|e_h\|_{L^2(\Omega)}$$

holds.

Proof. Using the continuity result in (5.3b), the result in Theorem 5.7 and the estimate (6.4) we obtain

$$\begin{aligned}
|A_h(z\circ\Phi_h - z_h, e_h\circ\Phi_h)| &\lesssim h^k\|z\circ\Phi_h - z_h\|_h\big(\|u\|_{H^{k+1}(\Omega_1\cup\Omega_2)} + \|f\|_{H^{1,\infty}(\Omega_1\cup\Omega_2)}\big) \\
&\lesssim h^{k+1}\big(\|u\|_{H^{k+1}(\Omega_1\cup\Omega_2)} + \|f\|_{H^{1,\infty}(\Omega_1\cup\Omega_2)}\big)\|e_h\|_{L^2(\Omega)}.
\end{aligned}$$

□

Lemma 6.3. *Let z_h be as in* (6.4). *The estimate*

$$|A_h(u\circ\Phi_h, z_h) - A(u, z_h\circ\Phi_h^{-1})| \lesssim h^{k+1}\|u\|_{H^2(\Omega_1\cup\Omega_2)}\|e_h\|_{L^2(\Omega)} \tag{6.5}$$

holds.

Proof. We use the splitting

$$\begin{aligned}
&A_h(u\circ\Phi_h, z_h) - A(u, z_h\circ\Phi_h^{-1})\\
&= A_h(u\circ\Phi_h, z_h - z\circ\Phi_h) - A(u, z_h\circ\Phi_h^{-1} - z) \qquad (6.6)\\
&+ A_h(u\circ\Phi_h, z\circ\Phi_h) - A(u, z). \qquad (6.7)
\end{aligned}$$

For the term in (6.6) we use the approximation result (5.13a) and (6.4):

$$\begin{aligned}
&|A_h(u\circ\Phi_h, z_h - z\circ\Phi_h) - A(u, z_h\circ\Phi_h^{-1} - z)| \lesssim h^k\|u\|_{H^2(\Omega_1\cup\Omega_2)}\|z_h - z\circ\Phi_h\|_h\\
&\lesssim h^{k+1}\|u\|_{H^2(\Omega_1\cup\Omega_2)}\|e_h\|_{L^2(\Omega)}.
\end{aligned}$$

For the term in (6.7) we use $[\![u]\!] = [\![z]\!] = 0$ and thus get:

$$\begin{aligned}
&A_h(u\circ\Phi_h, z\circ\Phi_h) - A(u, z)\\
&= \sum_{i=1}^{2}\alpha_i\Big(\int_{\Omega_{i,h}}\nabla(u\circ\Phi_h)\cdot\nabla(z\circ\Phi_h)\,dx - \int_{\Omega_i}\nabla u\cdot\nabla z\,dx\Big)\\
&= \sum_{i=1}^{2}\alpha_i\int_{\Omega_i} C\nabla u\cdot\nabla z\,dx,
\end{aligned}$$

with the matrix $C := \det(B^{-1})B^TB - I,\ B := D\Phi_h$. We have $C \neq 0$ only on $\Delta_h := U_{\delta_h}$, with $\delta_h = ch$, for suitable $c > 0$. Furthermore, $\|C\|_{\infty,\Omega} \lesssim h^k$ holds, cf. [24, Proof of Lemma 5.6]. Using this and Lemma 5.5 we obtain

$$\begin{aligned}
|A_h(u\circ\Phi_h, z\circ\Phi_h) - A(u, z)| &\lesssim h^k\|u\|_{H^1(\Delta_h)}\|z\|_{H^1(\Delta_h)}\\
&\lesssim h^{k+1}\|u\|_{H^2(\Omega_1\cup\Omega_2)}\|z\|_{H^2(\Omega_1\cup\Omega_2)}\\
&\lesssim h^{k+1}\|u\|_{H^2(\Omega_1\cup\Omega_2)}\|e_h\|_{L^2(\Omega)}.
\end{aligned}$$

Combing these results completes the proof. □

LEMMA 6.4. *Let z_h be as in* (6.4). *The estimate*

$$|f(z_h\circ\Phi_h^{-1}) - f_h(z_h)| \lesssim h^{k+1}\|f\|_{H^{1,\infty}(\Omega_1\cup\Omega_2)}\|e_h\|_{L^2(\Omega)} \qquad (6.8)$$

holds.

Proof. Using (5.13b) we get

$$|f(z_h\circ\Phi_h^{-1}) - f_h(z_h)\| \lesssim h^{k+1}\|f\|_{H^{1,\infty}(\Omega_1\cup\Omega_2)}\|z_h\|_h$$

Furthermore, using (6.4) we get

$$\|z_h\|_h \le \|z_h - z\circ\Phi_h\|_h + \|z\circ\Phi_h\|_h \lesssim h\|e_h\|_{L^2(\Omega)} + \|z\|_{H^2(\Omega_1\cup\Omega_2)} \lesssim \|e_h\|_{L^2(\Omega)}.$$

Thus we obtain the bound in (6.8). □

Combining the previous results we obtain the following main result.

THEOREM 6.5 (L^2-error bound). *We assume that the smoothness conditions on the solution u and on the data f, f_h as formulated in Theorem 5.7 are satisfied and that Γ and $\partial\Omega$ are sufficiently smooth such that we have the regularity property* (6.2)

for the solution of the problem (6.1). *The following bound holds for the discretization error:*

$$\begin{aligned}\|u - u_h \circ \Phi_h^{-1}\|_{L^2(\Omega)} &\simeq \|u \circ \Phi_h - u_h\|_{L^2(\Omega_h)} \\ &\lesssim h^{k+1}(\|u\|_{H^{k+1}(\Omega_1\cup\Omega_2)} + \|f\|_{H^{1,\infty}(\Omega_1\cup\Omega_2)}).\end{aligned} \tag{6.9}$$

7. Numerical experiment. Results of numerical experiments that confirm the optimal h^{k+1} convergence in the L^2-norm for the interface problem (2.1) are given in [22, 24]. However, In these examples the domain boundary is polygonal. In the experiment presented in this section we consider a case where the *curved* domain boundary is approximated by isoparametric elements.

The domain is a disk around the origin with radius $R = 2$, $\Omega = B_2((0,0))$. The domain is divided into an inner disk $\Omega_1 = B_1((0,0))$ and an outer ring $\Omega_2 = \Omega \setminus \Omega_1$. Hence, the interface is a circle described with the level set function $\phi(x) = \|x\|_2 - 1$, $\Gamma = \{\phi(x) = 0\}$. We approximate ϕ by $\phi_h \in V_h^k$ by interpolation. We set $(\alpha_1, \alpha_2) = (\pi, 2)$ and take the right hand-side f such that the exact solution is given by (with $r(x) = \|x\|_2$)

$$u(x) = \begin{cases} 2 + (\cos(\frac{\pi}{2} r(x)) - 1) & x \in \Omega_1, \\ 2 - r(x) & x \in \Omega_2. \end{cases} \tag{7.1}$$

Note that u fulfills the interface conditions. For the Nitsche stabilization parameter we choose $\lambda = 20k^2$ and measure the L^2 error on the curved mesh Ω_h which is obtained by applying the isoparametric mapping Θ_h. To measure the errors we use domain-wise the canonical extension of u leading to u^e as in (7.1) with Ω_i replaced by $\Omega_{i,h}$. Starting from a coarse initial mesh, see Figure 7.1 (top left), we apply three succesive mesh refinements and use polynomial degrees $k = 1, .., 5$. To solve the arising linear systems we used a direct solver. The method has been implemented in the add-on library `ngsxfem` to the finite element library `NGSolve` [31].

The results are shown in Figure 7.1. We observe the predicted optimal $\mathcal{O}(h^{k+1})$ behavior.

Acknowledgement. C. Lehrenfeld gratefully acknowledges funding by the German Science Foundation (DFG) within the project "LE 3726/1-1".

REFERENCES

[1] P. Bastian and C. Engwer, *An unfitted finite element method using discontinuous Galerkin*, International journal for numerical methods in engineering, 79 (2009), pp. 1557–1576.

[2] C. Bernardi, *Optimal finite-element interpolation on curved domains*, SIAM J. Numer. Anal., 26 (1989), pp. 1212–1240.

[3] T. Boiveau, E. Burman, S. Claus, and M. G. Larson, *Fictitious domain method with boundary value correction using penalty-free nitsche method*, arXiv preprint 1610.04482, (2016).

[4] S. Brenner and L. Scott, *The Mathematical Theory of Finite Element Methods*, Springer New York, 1994.

[5] E. Burman, P. Hansbo, and M. G. Larson, *A cut finite element method with boundary value correction*, arXiv preprint 1507.03096, (2015).

[6] K. W. Cheng and T.-P. Fries, *Higher-order XFEM for curved strong and weak discontinuities*, Int. J. Num. Meth. Eng., 82 (2010), pp. 564–590.

[7] C.-C. Chu, I. Graham, and T.-Y. Hou, *A new multiscale finite element method for high-contrast elliptic interface problems*, Math. of Computation, 79 (2010), pp. 1915–1955.

[8] K. Deckelnick, C. Elliott, and T. Ranner, *Unfitted Finite Element Methods using bulk meshes for surface partial differential equations*, SIAM Journal on Numerical Analysis, 52 (2014), pp. 2137–2162.

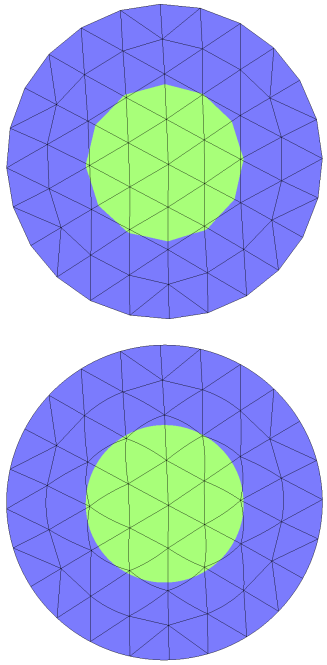

k	L	$\|u^e - u_h\|_{L^2(\Omega_h)}$	(eoc)
1	0	7.368×10^{-2}	(-)
	1	1.903×10^{-2}	(1.95)
	2	4.720×10^{-3}	(2.01)
	3	1.177×10^{-3}	(2.00)
2	0	5.534×10^{-3}	(-)
	1	5.858×10^{-4}	(3.24)
	2	6.384×10^{-5}	(3.20)
	3	7.703×10^{-6}	(3.05)
3	0	6.736×10^{-4}	(-)
	1	2.720×10^{-5}	(4.63)
	2	1.395×10^{-6}	(4.29)
	3	7.501×10^{-8}	(4.22)
4	0	9.318×10^{-5}	(-)
	1	1.285×10^{-6}	(6.18)
	2	2.630×10^{-8}	(5.61)
	3	6.248×10^{-10}	(5.40)
5	0	1.829×10^{-5}	(-)
	1	8.577×10^{-8}	(7.74)
	2	8.384×10^{-10}	(6.68)
	3	1.127×10^{-11}	(6.22)

FIG. 7.1. *Initial mesh with approximated geometry configuration Ω^{lin}, Ω_i^{lin} (top left) and isoparametrically mapped domain for $k = 2$ (bottom left). The table shows L^2-norm discretization errors on successively refined meshes and estimated orders of convergence.*

[9] K. Dréau, N. Chevaugeon, and N. Moës, *Studied X-FEM enrichment to handle material interfaces with higher order finite element*, Comput. Meth. Appl. Mech. Eng., 199 (2010), pp. 1922–1936.

[10] C. M. Elliott and T. Ranner, *Finite element analysis for a coupled bulk–surface partial differential equation*, IMA Journal of Numerical Analysis, 33 (2013), pp. 377–402.

[11] A. Ern and J.-L. Guermond, *Finite element quasi-interpolation and best approximation*, ESAIM:M2AN, 51 (2017), pp. 1367–1385.

[12] T.-P. Fries and S. Omerovi, *Higher-order accurate integration of implicit geometries*, Int. J. Num. Meth. Eng., (2015).

[13] J. Grande, C. Lehrenfeld, and A. Reusken, *Analysis of a high order trace finite element method for PDEs on level set surfaces*, Preprint arXiv:1611.01100, (2016). NAM preprint 2016-05. Accepted for publication in SIAM J. Numer. Anal. (2017).

[14] J. Grande and A. Reusken, *A higher order finite element method for partial differential equations on surfaces*, SIAM J. Numer. Anal., 54 (2016), pp. 388–414.

[15] S. Gross, V. Reichelt, and A. Reusken, *A finite element based level set method for two-phase incompressible flows*, Comput. Visual. Sci., 9 (2006), pp. 239–257.

[16] S. Gross and A. Reusken, *An extended pressure finite element space for two-phase incompressible flows*, J. Comput. Phys., 224 (2007), pp. 40–58.

[17] A. Hansbo and P. Hansbo, *An unfitted finite element method, based on Nitsches method for elliptic interface problems*, Computer Methods in Applied Mechanics and Engineering, 191 (2002), pp. 5537–5552.

[18] J. Huang and J. Zou, *Some new a priori estimates for second-order elliptic and parabolic interface problems*, Journal of Differential Equations, 184 (2002), pp. 570–586.

[19] F. Kummer and M. Oberlack, *An extension of the discontinuous Galerkin method for the singular poisson equation*, SIAM Journal on Scientific Computing, 35 (2013), pp. A603–A622.

[20] O. Ladyzhenskaya and N. Ural'tseva, *Linear and quasilinear equations of elliptic type*, Nauka, Moscow, 1973.

[21] P. L. Lederer, C.-M. Pfeiler, C. Wintersteiger, and C. Lehrenfeld, *Higher order un-*

fitted FEM for Stokes interface problems, PAMM, 16 (2016), pp. 7–10.

[22] C. Lehrenfeld, *High order unfitted finite element methods on level set domains using isoparametric mappings*, Computer Methods in Applied Mechanics and Engineering, 300 (2016), pp. 716 – 733.

[23] C. Lehrenfeld, *A higher order isoparametric fictitious domain method for level set domains*, arXiv preprint arXiv:1612.02561, (2016).

[24] C. Lehrenfeld and A. Reusken, *Analysis of a high order unfitted finite element method for elliptic interface problems*, IMA J. Numer. Anal., (2017). drx041, https://doi.org/10.1093/imanum/drx04.

[25] M. Lenoir, *Optimal isoparametric finite elements and error estimates for domains involving curved boundaries*, SIAM Journal on Numerical Analysis, 23 (1986), pp. 562–580.

[26] B. Müller, F. Kummer, and M. Oberlack, *Highly accurate surface and volume integration on implicit domains by means of moment-fitting*, Int. J. Num. Meth. Eng., 96 (2013), pp. 512–528.

[27] M. A. Olshanskii, A. Reusken, and J. Grande, *A finite element method for elliptic equations on surfaces*, SIAM Journal on Numerical Analysis, 47 (2009), pp. 3339–3358.

[28] P. Oswald, *On a BPX-preconditioner for $\mathbb{P}_1$ elements*, Computing, 51 (1993), pp. 125–133.

[29] J. Parvizian, A. Düster, and E. Rank, *Finite cell method*, Comput. Mech., 41 (2007), pp. 121–133.

[30] R. Saye, *High-order quadrature method for implicitly defined surfaces and volumes in hyperrectangles*, SIAM J. Sci. Comput., 37 (2015), pp. A993–A1019.

[31] J. Schöberl, *C++11 implementation of finite elements in NGSolve*, Tech. Report ASC-2014-30, Institute for Analysis and Scientific Computing, September 2014.

[32] Y. Sudhakar and W. A. Wall, *Quadrature schemes for arbitrary convex/concave volumes and integration of weak form in enriched partition of unity methods*, Computer Methods in Applied Mechanics and Engineering, 258 (2013), pp. 39–54.